The Transducer Protein HtrII Modulates the Lifetimes of Sensory Rhodopsin II Photointermediates

Jun Sasaki and John L. Spudich

Department of Microbiology and Molecular Genetics, University of Texas Medical School, Houston, Texas 77030 USA

ABSTRACT   We studied the photochemical reaction cycle of sensory rhodopsin II (SRII) by flash photolysis of *Halobacterium salinarum* membranes genetically engineered to contain or to lack its transducer protein HtrII. Flash photolysis data from membranes containing HtrII were fit well in the 10 μs–10 s range by three rate constants and a linear unbranched pathway from the unphotolyzed state with 487 nm absorption maximum to a species with absorption maximum near 350 nm (M) followed by a species with maximum near 520 nm (O), as has been found in previous studies of wild-type membranes. Data from membranes devoid of HtrII exhibited similar M and O intermediates but with altered kinetics, and a third intermediate absorbing maximally near 470 nm (N) was present in an equilibrium mixture with O. The modulation of SRII photoreactions by HtrII indicates that SRII and HtrII are physically associated in a molecular complex. Arrhenius analysis shows that the largest effect of HtrII, the acceleration of O decay, is attributable to a large decrease in activation enthalpy. Based on comparison of SRII photoreactions to those of sensory rhodopsin I and bacteriorhodopsin, we interpret this kinetic effect to indicate that HtrII interacts with SRII so that it alters the reaction process involving deprotonation of Asp[73], the proton acceptor from the Schiff base.

INTRODUCTION

Sensory rhodopsin II (SRII; Spudich et al., 1986) (also called phoborhodopsin; Tomioka et al., 1986) is one of four retinylidene proteins present in the membranes of the archaeon *Halobacterium salinarum*. Bacteriorhodopsin (BR) and halorhodopsin (HR) function as light-driven ion pumps for protons and chloride, respectively (Rothschild, 1992; Oesterhelt et al., 1992; Lanyi, 1997). Sensory rhodopsin I (SRI) and SRII are phototaxis receptors that transmit attractant and repellent signals, respectively, to their transducer proteins HtrI and HtrII, which in turn modulate a phosphotransfer cascade producing flagellar motor responses (Hoff et al., 1997). Despite their differing functions, the archaeal rhodopsins share a similar architecture, consisting of seven transmembrane α-helices surrounding a retinal chromophore that is covalently bound through a protonated Schiff base linkage to a lysine residue in the middle of the seventh helix. They also all exhibit similar cyclic photochemical reaction pathways (photocycles), in that photoisomerization of the all-*trans* retinal to the 13-*cis* configuration triggers conversion to spectroscopically distinct intermediates and final recovery of the initial state.

The photocycle reactions have been most extensively studied in BR (λ_{max} 568 nm), which exhibits sequential intermediates named K, L, M, N, and O. In M formation, the protonated Schiff base on helix G donates its proton to its primary counterion Asp[85] on helix C. M has a strongly

blue-shifted absorption maximum at 412 nm due to the deprotonation of the Schiff base. The protonation of Asp[85] then induces proton release from Glu[204] and possibly Glu[194] to the periplasmic side of the membrane (Brown et al., 1995; Balashov et al., 1997; Dioumaev et al., 1998). The breakage of the interhelical salt bridge between Asp[85] and the Schiff base by the proton transfer drives the opening of the cytoplasmic channel, causing the hydration of Asp[96] to release its proton and reprotonate the Schiff base in N formation (Subramaniam et al., 1993; Kamikubo et al., 1996). In O, the retinal configuration is returned to the all-*trans* form, but Asp[85] is still protonated, giving rise to a spectrum red-shifted relative to the original state (Bousche et al., 1992; Kandori et al., 1997). SRII contains the interhelical salt bridge between the protonated Schiff base and the counterion Asp[73] (Spudich et al., 1997; Zhu et al., 1997), corresponding to Asp[85] in BR, but lacks the acidic residues corresponding to Glu[194], Glu[204], and Asp[96] of BR (Zhang et al., 1996).

A major difference between the light-driven ion pumps (BR and HR) and photoreceptors (SRI and SRII) is that the latter associate with transducer proteins (HtrI and HtrII). HtrI (Yao and Spudich, 1992) and HtrII (Zhang et al., 1996) are homologous to eubacterial methyl-accepting chemotaxis transducers (Falke et al., 1997). They are each made up of two transmembrane helices, connected to cytoplasmic methylation and signaling domains and a short (HtrI) and long (HtrII) periplasmic domain. Their signaling domains control the activity of a histidine kinase that phosphorylates a flagellar motor-regulator protein (Rudolph et al., 1995). HtrI has been shown to be a dimer by cross-linking of engineered disulfides (Zhang and Spudich, 1998), and presumably HtrII is also dimeric.

The binding of HtrI to SRI has large kinetic effects on the SRI photocycle, which provided the initial evidence that the

two proteins were bound in a molecular complex (Spudich and Spudich, 1993; Krah et al., 1994). In the presence of HtrI the M intermediate of SRI, S_{373}, forms with a half-time of 300 μs and returns thermally to the unphotolyzed state, SR_{587}, with a half-time of 800 ms (23°C) (Bogomolni and Spudich, 1987). In the absence of HtrI the rise of M after photoexcitation of SR_{587} is ~30 times slower (10 ms), and the decay of M at neutral pH is also very slow (6 s) (see discussion in Hoff et al., 1997). The rate of M decay, which requires reprotonation of the Schiff base, is insensitive to pH over a broad range (pH 4–8) in the SRI-HtrI complex, whereas HtrI-free SRI M decay is strongly pH sensitive, varying from 80 ms to >10 s in the same range (Spudich and Spudich, 1993). These kinetic effects have been interpreted in terms of HtrI binding preventing the opening of a proton-conducting channel from the cytoplasm to the photoactive center of SRI (Spudich, 1994), which is supported by the light-induced exchange of protons with the aqueous phase by SRI that is blocked by HtrI (Olson and Spudich, 1993) and the light-driven proton transport by SRI, also blocked by HtrI (Bogomolni et al., 1994).

Given the analogous functions of SRII and SRI, similar modulation of the SRII photocycle by HtrII binding might be expected. However, there are significant differences between the two receptors in the proton transfer reactions sensitive to HtrI binding in SRI. In SRI the Asp^{76} residue that corresponds to the Schiff base counterion Asp^{73} in SRII is protonated in the initial SR_{587} state, and therefore Asp^{76} is not the proton acceptor from the Schiff base during the process of M formation (Rath et al., 1996). SRII, in contrast, has an unprotonated Asp^{73} serving as the primary counterion to the protonated Schiff base and as the proton acceptor during SRII M formation (Spudich et al., 1997; Zhu et al., 1997). Furthermore, in SRI reprotonation of the Schiff base occurs in the final spectral transition in the photocycle, whereas in SRII reprotonation is an intermediate event (Tomioka et al., 1986). In the work reported here we have tested for modulation of each step of the SRII photocycle by HtrII to better understand these differences and the relationship of SRII photocycle transformations to its signaling via interaction with HtrII.

MATERIALS AND METHODS

Membrane preparation

Transformed *H. salinarum* membranes containing SRII in the absence and presence of HtrII were produced by plasmid expression in the SRII⁻HtrII⁻ mutant Pho81Wr⁻, which also lacks the other three archaeal rhodopsins (BR, HR, and SRI), as described (Spudich et al., 1997; Zhu et al., 1997). Expression of HtrII-free SRII used the highly efficient *bop* promoter, whereas expression of the SRII-HtrII complex used the *htrI* promoter placed in front of the *htrII-sopII* gene pair. This construction produces the complex at higher levels than the *htrII* promoter. Membranes were prepared by sonication as described (Spudich and Spudich, 1993). In the final step before use in this study, the membranes were pelleted by centrifugation at 48,000 rpm (Beckman, rotor type 70 Ti) for 60 min at 4°C and resuspended in 25 mM Tris buffer (pH 6.8) containing 4 M NaCl.

Flash photolysis

Flash-induced absorption transients in the microsecond and millisecond time domains were acquired on an Olis RSM-1000 and a Nicolet Integra20 digital oscilloscope, respectively, after a Nd-YAG laser flash (532 nm, 6 ns, 40 mJ) in a laboratory-constructed flash photolysis system. For calculation of the amplitude spectra of the exponentially decaying components with different rate constants, 26 absorption transients were collected from 600 to 350 nm at 10-nm intervals. Each trace was obtained by averaging 32–128 acquisition sweeps. The measurements were made at 490, 360, and 540 nm for optimal detection of the initial state, the species with unprotonated Schiff base (M), and the species with red-shifted absorption spectrum (O), respectively.

Calculation of the amplitude spectra

The 26 time-dependent traces were subjected to singular value decomposition, which gave 26 spectra (*U* spectra), each with the corresponding weight factor (singular value *S*) to be multiplied by it, and with a time-dependent trace (*V* vector) representing the time-dependent transient of the amplitude of each spectrum (Hug et al., 1990; Sasaki et al., 1994, 1995). The number of the kinetic components (*n*) present in the photoreaction process was deduced from the number of *U* spectra or *V* vectors that exceeded the noise level. All of the *V* vectors above noise level (V_1 to V_n) were fitted with *n* exponentials. For example, the *i*th vector (V_i) was fitted with $\sum_{j=1}^{n} A_{ij}\exp(k_j t)$. The amplitude spectra of each of the *j*th exponential components was calculated as $\sum_{i=1}^{n} U_i \times S_i \times A_{ij}$ as described (Hug et al., 1990; Sasaki et al., 1994, 1995).

RESULTS AND DISCUSSION

HtrII modulates the kinetics of the photocycle of SRII

To examine the effect of HtrII on SRII, we compared the absorption transients in the photocycle of SRII at times more than 10 μs after photoexcitation in the absence and presence of HtrII. The absorbance transients most sensitive to the formation of the M intermediate with putatively deprotonated Schiff base were monitored at 360 nm, at pH 6.8, 4 M NaCl, and 35°C (Fig. 1 *a*). In HtrII-free SRII, M rises with a half-time of 10 μs. The rate is retarded when HtrII is present with SRII to 36 μs (Fig. 1 *b*). The later points used for the fits as shown in the figure are the most reliable in the data, because a flash artifact may have influenced earlier values in the traces. Because the counterion of the protonated Schiff base in SRII is Asp^{73} (Zhu et al., 1997), and Schiff base deprotonation is blocked in the D73N mutant (Spudich et al., 1997), we concluded that M formation involves proton transfer from the Schiff base to Asp^{73}. A carboxylate protonation band evident in light-dark Fourier transform infrared spectra of SRII from *Natronobacterium pharaonis* further supports this conclusion (Engelhard et al., 1995). Therefore our interpretation is that HtrII is associated with SRII, and this association modulates the proton transfer reaction from the Schiff base to Asp^{73} in the interior of SRII.

Fig. 2 shows absorbance transients of SRII in the absence (Fig. 2 *a*) and presence (Fig. 2 *b*) of HtrII recorded at 360, 490, and 540 nm in the ms to 8-s time window measured at 35°C. M behavior is monitored at 360 nm, and that of the
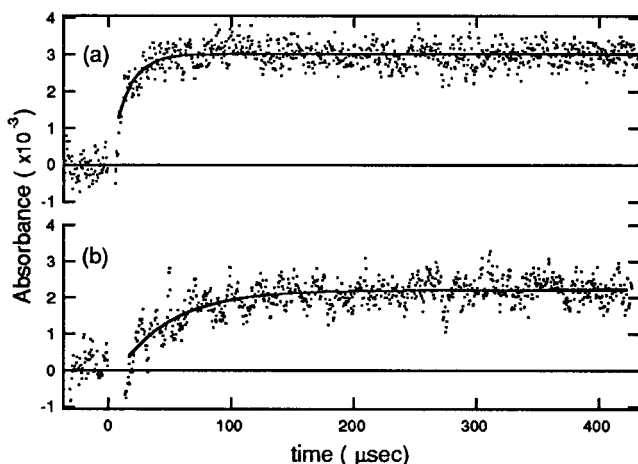
FIGURE 1   Flash-induced absorption transients at 360 nm of SRII in the absence (*a*) and in the presence (*b*) of HtrII. 532-nm laser flash was at $t = 0$. Measurements were made with membranes in 25 mM Tris-HCl buffer (pH 6.8), 4 M NaCl, and at 35°C. Negative values from a flash artifact of $0-10$ μs and $0-20$ μs have been deleted from the data for *a* and *b*, respectively.

red-shifted intermediate (O) at 540 nm. The data for SRII in the presence of HtrII showing a half-time for M decay and O rise of 30 ms and decay of O in 170 ms (Fig. 2 *b*) is in keeping with the analysis of wild type in the first study of the SRII photocycle (Tomioka et al., 1986), taking into account the lower temperature (20°C) used in that study. We measured slower rates of M decay and O rise and decay in the absence of HtrII (Fig. 2 *a*). In the HtrII-free SRII photocycle, M decays with a 66-ms half-time simultaneously with the rise of absorption at 540 nm, showing that M is converted to O. O then returns to $SRII_{487}$ with a 1.0-s
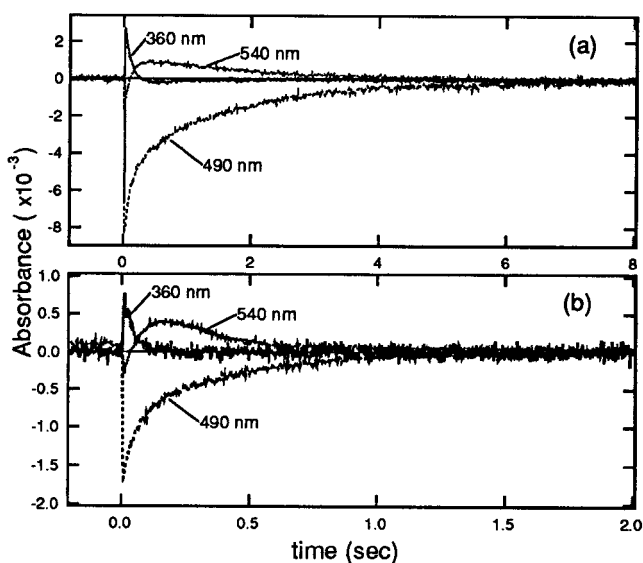

FIGURE 2   Flash-induced absorption transients of SRII in the absence (*a*) and in the presence (*b*) of HtrII in times greater than milliseconds. Conditions are as in Fig. 1. Note the 4× expanded time axis in *b* compared to *a*.

half-time evident both in the decay of the absorbance at 540 nm and the recovery at 490 nm (Fig. 2 *a*).

The long lifetime of O may be attributable to the absence of carboxylate groups at positions 194 and 204 of BR, which are replaced by Ala and Tyr in SRII, respectively. The side chains of these residues in BR apparently form part of the proton release path, because in the mutants E204Q and E194Q, proton release is delayed until the end of the photocycle. O decay, which requires Asp[85] deprotonation, is retarded in E204Q and E194Q (Brown et al., 1995; Dioumaev et al., 1998). The similar red-shifted absorption maximum of the O intermediate in SRII argues that the Schiff base is reprotonated during M decay, with Asp[73] remaining protonated until the end of the photocycle, releasing its proton with O decay. This picture is in agreement with our preliminary observation for HtrII-free SRII by pyranine measurements as described for SRI (Olson and Spudich, 1993), which demonstrate proton uptake from the medium with M decay (O formation) and release with O decay (data not shown).

In the presence of HtrII there is an increased amplitude of the 540-nm trace relative to the 360-nm and 490-nm traces (Fig. 2 *b*) as compared to those in the free SRII photocycle (Fig. 2 *a*). The rate of the M-to-O conversion is slightly higher in the presence than in the absence of HtrII, and the rate of O decay to $SRII_{487}$ (170 ms) is greatly accelerated over the 1.0-s value for transducer-free SRII.

The above results show that the presence of HtrII modulates the rate of formation and decay of the intermediates in the SRII photocycle. Similarly, HtrI presence in the membrane modulates M formation (Jung et al., manuscript in preparation) and decay (Spudich and Spudich, 1993) in SRI. In that case, there is compelling evidence that SRI and HtrI are physically interacting in a molecular complex. Most directly, HtrI copurifies with His-tagged SRI during nickel-affinity chromatography (Spudich and Spudich, unpublished result). Our interpretation from the results here is that SRII and HtrII also form a molecular complex.

HtrII affects the equilbrium between late photocycle intermediates of SRII

For investigating spectral features of the intermediates, the same measurements as in Fig. 2 were performed across the spectrum between 350 and 600 nm at 10-nm intervals for SRII in the absence and presence of HtrII. The number of kinetic components involved in the reaction process was deduced by subjecting the sets of 26 traces to singular value decomposition (SVD). The result of SVD provided 26 spectra, corresponding weight factors, and time-dependent traces, with only the first two of them above noise level, indicating that the photocycle at ≥ms times involves two kinetic components as noted above as M-to-O conversion and O decay. The traces can be separated into two exponential components with rate constants corresponding to the decay rates of M and O, and the amplitude spectra of the

two exponential components were calculated from the resultant spectra of SVD. The amplitude spectra for the first and second exponential components in the photocycle of free SRII that have time constants of 66 ms and 1 s, respectively, are shown in Fig. 3, *b* and *c*, with the appearing and the decaying components represented as positive and negative values, respectively. The spectrum in Fig. 3 *b* represents the spectral change that occurs with a half-life of 66 ms. The spectrum shows that the species absorbing near 350 nm (M) is converted to another species absorbing near 500 nm. The width of this band indicates formation of more than one species, evidently in rapid equilibrium, because a single rate constant characterizes this spectral change. We tentatively attribute this to the equilibrium of N and O, and therefore we interpret Fig. 3 *b* as corresponding to the difference spectrum of $M \rightarrow (N + O)$. The equilibrium is then converted back to the unphotolyzed $SRII_{487}$ in 1 s; Fig. 3 *c* corresponds to the difference spectrum for $(N + O) \rightarrow SRII_{487}$. The inversion of the sum of the spectra in Fig. 3, *b* and *c*, produces the difference spectrum for $SRII_{487} \rightarrow M$ (Fig. 3 *a*).

The absorption maximum of M of SRII is more greatly blue-shifted compared to the corresponding unprotonated Schiff base species of BR (M_{412}) and SRI (S_{373}). This may reflect the molecular mechanism of SRII for tuning the absorption maximum to establish the considerable blue shift of the absorption maximum of the unphotolyzed form of SRII relative to BR and SRI (Takahashi et al, 1990).

In a similar manner, the amplitude spectrum of each exponential component was obtained for SRII in the presence of HtrII. In this case also, SVD produced only two spectra and two time traces above noise level. The spectral change with a half-life of 30 ms corresponds to the disappearance of a species absorbing near 350 nm (M) and an increase in the absorbance near 520 nm (Fig. 3 *e*). Because the absorption band generated is not as broad as the one in the free SRII photocycle and its width is consistent with a single species, our interpretation is that the equilibrium of N and O is strongly biased toward O, so that the population in N is very small. The difference spectrum of the conversion that occurs with a 170-ms half-life time (Fig. 3 *f*) shows that O returns to the original state. The inversion of the sum of the spectra in Fig. 3, *e* and *f*, produces the difference spectrum for $SRII_{487} \rightarrow M$ (Fig. 3 *d*) and is nearly identical to that of free SRII (Fig. 3 *a*).

Effect of HtrII on thermodynamic parameters of SRII photocycle reactions

The most noticeable effects of HtrII on the reaction cycle of SRII other than the elimination of N is the retardation of the M rise and the acceleration of the kinetics of M and O decay. To interpret the effects in terms of thermodynamic parameters, the rate constants of M rise, M decay (O rise), and O decay were measured at 20, 25, 30, 35, and 40°C in the free and complexed SRII photocycle, and the natural
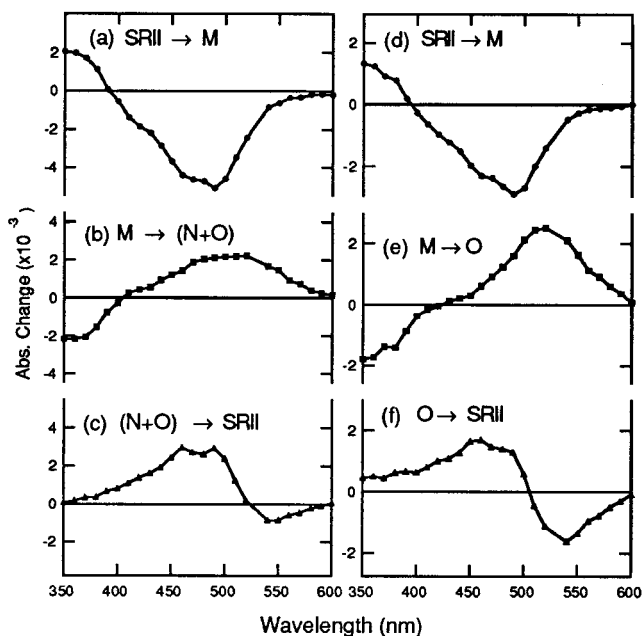
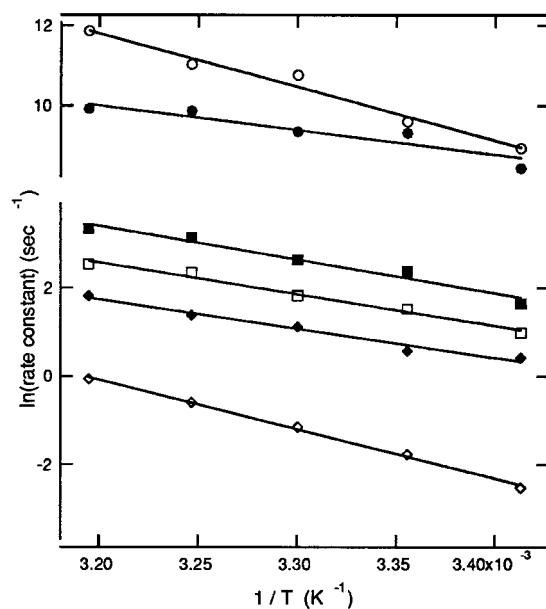FIGURE 3 Amplitude spectra of the exponentially decaying components after the excitation of free SRII (*a–c*) and HtrII-complexed SRII (*d–f*) in 25 mM Tris-Cl buffer (pH 6.8), 4 M NaCl, and at 35°C. Plotted values are maximum amplitudes of absorbance changes calculated from exponential fits to the V vectors produced by SVD. (*a* and *d*) Inversion of the sum *b* + *c* and *e* + *f*, respectively. (*b* and *e*) Absorption difference spectra of the 66-ms and 30-ms decaying components, respectively. (*c* and *f*) Absorption difference spectra of the 1.0-s and 170-ms decaying components, respectively.

FIGURE 4 Temperature dependence of the rate constants of M formation (○, −HtrII; ●, +HtrII), M-to-O conversion (□, −HtrII; ■, +HtrII), and O decay (◇, −HtrII; ◆, +HtrII). The rate constants were obtained by exponential fitting of the traces at 360 nm (for the rise and decay of M) and at 540 nm (for the decay of O) measured at 20, 25, 30, 35, and 40°C, and the natural logarithm of the rates were plotted against $1/T$.

TABLE 1　Activation enthalpy ($\Delta H^{\#}$) and activation entropy ($\Delta S^{\#}$) of M formation, M-to-O conversion, and O decay for SRII in the absence and presence of HtrII calculated from the fit of the plots in Fig. 4

	M-rise		M-to-O		O-decay	
	Free	Complex	Free	Complex	Free	Complex
$\Delta H^{\#}$ (kJ/mol)	105.6 ± 9.2	46.6 ± 7.5	55.9 ± 3.0	59.7 ± 6.8	88.3 ± 3.0	49.4 ± 3.4
$\Delta S^{\#}$ (J/mol · K)	193.9 ± 32.1	−9.4 ± 24.2	−40.1 ± 10.1	−21.3 ± 22.5	42.1 ± 10.0	−67.8 ± 11.7

logarithms of the rates were plotted against the reciprocal of the temperatures (Fig. 4). Each plot fit well to a single line, confirming the validity of separating the kinetics into three components in the photocycle in $>\mu s$ times. Activation enthalpy ($\Delta H^{\#}$) and activation entropy ($\Delta S^{\#}$) of each kinetic component were given by the fit of each plot with the equation

$$\ln k = \ln(k_B T/h) - \Delta H^{\#}/RT + \Delta S^{\#}/R,$$

where h is Planck's constant (6.6262×10^{-34} Js), k_B is Boltzmann's constant (1.38066×10^{-23} J/K), and R is the gas constant (8.3144 J/kmol). The derived $\Delta H^{\#}$ and $\Delta S^{\#}$ for M formation, M-to-O conversion, and O decay in the SRII photocycles in the absence and presence of HtrII are listed in Table 1.

The $\Delta H^{\#}$ for M formation in the free SRII is reduced by about half when complexed with HtrII. However, the activation free energy ($\Delta G^{\#} = \Delta H^{\#} - T\Delta S^{\#}$) for this reaction shows a net increase in the complex because of the considerable decrease in $\Delta S^{\#}$ which is the main contributor to the retardation of M formation in the complex. For the M-to-O conversion kinetics, $\Delta H^{\#}$ values in the free and complexed SRII photocycles are almost unchanged, as can be judged from the parallel feature of the plots of their M-decay kinetics. The effects of HtrII complexation on $\Delta H^{\#}$ and $\Delta S^{\#}$ are relatively small. Although the values listed in Table 1 contain some ambiguity, acceleration by HtrII binding seems to be attributable more to the increase in $\Delta S^{\#}$ than to the decrease in $\Delta H^{\#}$. If the acceleration comes from an entropic effect, HtrII binding possibly constrains the SRII molecule, so that the extent of helix movements occurring in M and N (in helices B, G, and F in BR; Kamikubo et al., 1996) is less. Such an effect may accelerate both M and N decays, explaining as well the absence of N from the photocycle of the complex.

Acceleration of O-decay by HtrII is brought about by a decrease in $\Delta H^{\#}$ to about half. Significant reductions in $\Delta H^{\#}$ by HtrII interaction is observed in the formation of M and the decay of O, both of which are related to proton transfers involving Asp[73]: from the Schiff base to Asp[73] (M formation) and from Asp[73] to an unidentified acceptor, possibly bulk water in the medium (O decay). Therefore, evidently the bound HtrII influences the hydrogen-bonding network on the extracellular side of SRII, where Asp[73] is located. The reduction in the $\Delta H^{\#}$ in these processes when SRII is complexed with HtrII may involve a change in hydrogen-bonding interactions around Asp[73] so as to make the proton transfers more rapid. Similar modulation of the kinetics was observed in the SRI and HtrI complex for the decay of the M-like intermediate, S_{373} (Yan et al., 1997), indicating that HtrI binding changes the hydrogen-bonding network around the Schiff base to facilitate its protonation. Because S_{373} is a signaling state in the SRI photocycle, the similar modulation of O decay (and to a lesser extent M decay) in SRII by HtrII suggests that O, as well as M, is a signaling state. A retinal analog study also supports SRII O as maintaining a signaling conformation formed in M (Yan et al., 1991).

In summary: HtrII binding to SRII has substantial effects on the photocycle of SRII by influencing the molecule on both its extracellular and cytoplasmic sides. On the extracellular side HtrII facilitates proton transfers around the Schiff base and Asp[73], and on the cytoplasmic side, it apparently constrains the molecule to destabilize the structure of M and N, in which a global conformational change is expected to have occurred.

REFERENCES

Balashov, S. P., E. S. Imasheva, T. G. Ebrey, N. Chen, D. R. Menick, and R. K. Crouch. 1997. Glutamate-194 to cysteine mutation inhibits fast light-induced proton release in bacteriorhodopsin. *Biochemistry*. 36: 8671–8676.

Bogomolni, R. A., and J. L. Spudich. 1987. The photochemical reactions of bacterial sensory rhodopsin. I. Flash photolysis study in the one microsecond to eight second time window. *Biophys. J.* 52:1071–1075.

Bogomolni, R. A., W. Stoeckenius, I. Szundi, E. Perozo, K. D. Olson, and J. L. Spudich. 1994. Removal of transducer HtrI allows electrogenic proton translocation by sensory rhodopsin I. *Proc. Natl. Acad. Sci. USA*. 91:10188–10192.

Bousche, O., S. Sonar, M. P. Krebs, H. G. Khorana, and K. J. Rothschild. 1992. Time-resolved Fourier transform infrared spectroscopy of the bacteriorhodopsin mutant Tyr-185→Phe: Asp-96 reprotonates during O formation; Asp-85 and Asp-212 deprotonate during O decay. *Photochem. Photobiol.* 56:1085–1095.

Brown, L. S., J. Sasaki, H. Kandori, A. Maeda, R. Needleman, and J. K. Lanyi. 1995. Glutamic acid 204 is the terminal proton release group at the extracellular surface of bacteriorhodopsin. *J. Biol. Chem.* 270: 27122–27126.

Dioumaev, A. K., H. T. Richter, L. S. Brown, M. Tanio, S. Tuzi, H. Saitô, Y. Kimura, R. Needleman, and J. K. Lanyi. 1998. Existence of a proton transfer chain in bacteriorhodopsin: participation of Glu-194 in the release of protons to the extracellular surface. *Biochemistry*. 37: 2496–2506.

Engelhard, M., B. Scharf, and F. Siebert. 1995. Protonation changes during the photocycle of sensory rhodopsin II from *Natronobacterium pharaonis*. *FEBS Lett.* 395:195–198.

Falke, J. J., R. B. Bass, S. L. Butler, S. A. Chervitz, and M. A. Danielson. 1997. The two-component signaling pathway of bacterial chemotaxis: a molecular view of signal transduction by receptors, kinases, and adaptation enzymes. *Annu. Rev. Cell Dev. Biol.* 13:457–512.

Hoff, W. D., K.-H. Jung, and J. L. Spudich. 1997. Molecular mechanism of photosignaling by archaeal sensory rhodopsins. *Annu. Rev. Biophys. Biomol. Struct.* 26:223–258.

Hug, S. J., J. W. Lewis, C. M. Einterz, T. E. Thorgeirsson, and D. S. Kliger. 1990. Nanosecond photolysis of rhodopsin: evidence for a new, blue-shifted intermediate. *Biochemistry.* 29:1475–1485.

Kamikubo, H., M. Kataoka, G. Váró, T. Oka, F. Tokunaga, R. Needleman, and J. K. Lanyi. 1996. Structure of the N intermediate of bacteriorhodopsin revealed by x-ray diffraction. *Proc. Natl. Acad. Sci. USA.* 93: 1386–1390.

Kandori, H., Y. Yamazaki, M. Hatanaka, R. Needleman, L. S. Brown, T. H. Richter, J. K. Lanyi, and A. Maeda. 1997. Time-resolved Fourier transform infrared study of structural changes in the last steps of the photocycles of Glu-204 and Leu-93 mutants of bacteriorhodopsin. *Biochemistry.* 36:5134–5141.

Krah, M., W. Marwan, A. Vermeglio, and D. Oesterhelt. 1994. Phototaxis of *Halobacterium salinarium* requires a signaling complex of sensory rhodopsin I and its methyl-accepting transducer HtrI. *EMBO J.* 13: 2150–2155.

Lanyi, J. K. 1997. Mechanism of ion transport across membranes. Bacteriorhodopsin as a prototype for proton pumps. *J. Biol. Chem.* 272: 31209–31212.

Oesterhelt, D., J. Tittor, and E. Bamberg. 1992. A unifying concept for ion translocation by retinal proteins. *J. Bioenerg. Biomembr.* 24:181–191.

Olson, K. D., and J. L. Spudich. 1993. Removal of the transducer protein from sensory rhodopsin I exposes sites of proton release and uptake during the receptor photocycle. *Biophys. J.* 65:2578–2585.

Rath, P., E. N. Spudich, D. D. Neal, J. L. Spudich, and K. J. Rothschild. 1996. Asp[76] is the Schiff base counterion and proton acceptor in the proton-translocating form of sensory rhodopsin I. *Biochemistry.* 35: 6690–6696.

Rothschild, K. J. 1992. FTIR difference spectroscopy of bacteriorhodopsin: toward a molecular model. *J. Bioenerg. Biomembr.* 24:147–167.

Rudolph, J., N. Tolliday, C. Schmitt, S. C. Schuster, and D. Oesterhelt. 1995. Phosphorylation in halobacterial signal transduction. *EMBO J.* 14:4249–4257.

Sasaki, J., J. K. Lanyi, R. Needleman, T. Yoshizawa, and A. Maeda. 1994. Complete identification of C=O stretching vibrational bands of protonated aspartic acid residues in the difference infrared spectra of M and N intermediates versus bacteriorhodopsin. *Biochemistry.* 33:3178–3184.

Sasaki, J., T. Yuzawa, H. Kandori, A. Maeda, and H. Hamaguchi. 1995. Nanosecond time-resolved infrared spectroscopy distinguishes two K species in the bacteriorhodopsin photocycle. *Biophys. J.* 68:2073–2080.

Spudich, J. L. 1994. Protein-protein interaction converts a proton pump into a sensory receptor. *Cell.* 79:747–750.

Spudich, E. N., M. Sheves, G. Steinberg, and J. L. Spudich. 1997. Complexation of the signal transducing protein HtrI to sensory rhodopsin I and its effect on thermodynamics of signaling state deactivation. *J. Phys. Chem.* 101:109–113.

Spudich, E. N., and J. L. Spudich. 1993. The photochemical reactions of sensory rhodopsin I are altered by its transducer. *J. Biol. Chem.* 268: 16095–16097.

Spudich, E. N., S. A. Sundberg, D. Manor, and J. L. Spudich. 1986. Properties of a second sensory receptor protein in *Halobacterium halobium*. *Proteins.* 1:239–246.

Spudich, E. N., W. Zhang, M. Alam, and J. L. Spudich. 1997. Constitutive signaling of the phototaxis receptor sensory rhodopsin II from disruption of its protonated Schiff base-Asp[73] salt bridge. *Proc. Natl. Acad. Sci. USA.* 94:4960–4965.

Subramaniam, S., M. Gerstein, D. Oesterhelt, and R. Henderson. 1993. Electron diffraction analysis of structural changes in the photocycle of bacteriorhodopsin. *EMBO J.* 12:1–8.

Takahashi, T., B. Yan, P. Mazur, F. Derguini, K. Nakanishi, and J. L. Spudich. 1990. Color regulation in the archaebacterial phototaxis receptor phoborhodopsin (sensory rhodopsin II). *Biochemistry.* 29: 8467–8474.

Tomioka, H., T. Takahashi, N. Kamo, and Y. Kobatake. 1986. Flash spectrophotometric identification of a fourth rhodopsin-like pigment in *Halobacterium halobium*. *Biochem. Biophys. Res. Commun.* 139: 389–395.

Yan, B., T. Takahashi, R. Johnson, and J. L. Spudich. 1991. Identification of signaling states of a sensory receptor by modulation of lifetimes of stimulus-induced conformations: the case of sensory rhodopsin II. *Biochemistry.* 30:10686–10692.

Yan, B., E. N. Spudich, M. Sheves, G. Steinberg, and J. L. Spudich. 1997. Complexation of the signal transducing protein HtrI to sensory rhodopsin I and its effect on thermodynamics of signaling state deactivation. *J. Phys. Chem.* 101:109–113.

Yao, V. J., and J. L. Spudich. 1992. Primary structure of an archaebacterial transducer, a methyl-accepting protein associated with sensory rhodopsin I. *Proc. Natl. Acad. Sci. USA.* 89:11915–11919.

Zhang, W., A. Brooun, M. M. Mueller, and M. Alam. 1996. The primary structures of the archaeon *Halobacterium salinarium* blue light receptor sensory rhodopsin II and its transducer, a methyl-accepting protein. *Proc. Natl. Acad. Sci. USA.* 93:8230–8235.

Zhang, X.-N., and J. L. Spudich. 1998. HtrI is a dimer whose interface is sensitive to receptor photoactivation and His-166 replacements in sensory rhodopsin I. *J. Biol. Chem.* 273:19722–19728.

Zhu, J., E. N. Spudich, M. Alam, and J. L. Spudich. 1997. Effects of substitutions D73E, D73N, D103N and V106M on signaling and pH titration of sensory rhodopsin II. *Photochem. Photobiol.* 66:788–791.